International Journal of Heat and Technology
Vol. 40, No. 1, February, 2022, pp. 91-97
Journal homepage: http://iieta.org/journals/ijht

Thermal Stress Analysis and Structural Optimization of High-Rise Buildings under Stack Effect

Cheng Huang[1], Juan Chen[2*]

[1] School of Art, Anhui Jianzhu University, Hefei 230022, China
[2] Art Design Department, Anhui University of Arts, Hefei 230001, China

Corresponding Author Email: ahysxyrsc@ahua.edu.cn

https://doi.org/10.18280/ijht.400111

Received: 2 November 2021
Accepted: 5 January 2022

Keywords:
stack effect, high-rise buildings, thermal stress analysis, structural optimization

ABSTRACT

Thermal stress and thermal strain are the major causes of wall cracking of high-rise buildings. The key to wall cracking control lies in regulating thermal stress, and reducing the uncoordinated deformation probability of structural members. However, the existing studies have not considered the common stack effect of high-rise buildings. To fill up the gap, this paper analyzes the thermal stress and optimizes the structure of high-rise buildings under stack effect. Firstly, the cracking mechanism of structural members in high-rise buildings was expounded under stack effect, and the thermal stress of these buildings was analyzed in the light of that effect. Next, finite-element calculation was performed on the instantaneous stress field of high-rise buildings. After that, the thermal stress of high-rise buildings was fully analyzed. Several suggestions were provided for the structural design and optimization of high-rise buildings.

1. INTRODUCTION

High-rise buildings continue to emerge with the increase in population and the development of construction engineering technology [1-9]. However, the structural functionality and safety of some high-rise buildings are challenged by cracking, which calls for repair and maintenance [10-12]. The cracking of structural members in high-rise buildings may arise from various factors. Thermal stress and thermal strain are the major causes of wall cracking of high-rise buildings [13-18]. Thus, the key to wall cracking control lies in regulating thermal stress, and reducing the uncoordinated deformation probability of structural members [19-22]. To reduce thermal stress, lower thermal strain, and prevent cracking, domestic and foreign experts and researchers have long been exploring several problems: how to fully consider the effect of thermal stress on structural design and optimization of high-rise buildings, and how to effectively control the internal and external temperatures during building maintenance.

The pouring of a large volume of concrete generates a huge amount of heat. The resulting thermal cracks reduces the structural stiffness. Guo [23] briefly introduced the thermal conduction principle of solids and the reasons for thermal cracking, and simulated large volume concrete on COMSOL. The results show that the simulation model is reliable enough to analyze temperature variation. Russell [24] carried out a series of experiments on a 12-layer reduced scale building model, and investigated the temperature of fire rooms in high-rise buildings under stack effect. In addition, the mass loss rate of fuel, radiation flux, heat flow, and temperature of the atrium and fire rooms were discussed based on the experimental data. The research findings provide a reference for the safety design of the rooms in high-rise buildings.

During the design of reinforced concrete high-rise buildings, it is necessary to consider the length variation of the vertical members with the elapse of time. In the context of actual stress history and actual material properties, Russell [24] considered instantaneous deformation, shrinkage deformation, and creep deformation, predicted the shrinkage of vertical members in high-rise buildings accurately, and pointed out the daily and seasonal changes of temperature. The exposed parts of buildings respond to the temperature changes via induction force or deformation, which depends on the degree of exposure and the boundary condition of the structural members. Khan and Fintel [25] described the structural details of high-rise buildings to avoid damages from the deformation difference caused by the temperature disparity between internal and external columns.

Due to the differences in steel bars and sizes, the vertical load bearing members may differ in creep and shrinkage. The ensuing problems can be minimized through proper structural design and detailed design. Kahsay and Bitsuamlak [26] surveyed the effects of these parameters on the energy consumption of rooms at different locations. These rooms, which are part of a 100 m-tall high-rise building, were exposed to different weather conditions, and designed with different window-to-wall ratios (WWRs). The results show that, for a high-rise building exposed in a windy microclimate with 100% WWR, the differences in annual energy consumptions of heating and cooling were 11.2% and 4.7%, respectively.

After summing up the existing results on the temperature field and thermal stress of structural members in high-rise buildings, the authors found that the relevant studies have provided simplified assumptions and approximate solutions for the thermal stress on the structural members in high-rise buildings, containing complex circulation spaces. However, none of them have considered the common stack effect in high-rise buildings. Therefore, this paper analyzes the thermal stress of high-rise buildings under stack effect, and provides suggestions on structural optimization. Section 2 expounds on the cracking mechanism of structural members in high-rise buildings under stack effect, and analyzes the thermal stress of such buildings under stack effect. Section 3 completes the finite-element calculation on the instantaneous stress field of high-rise buildings. Section 4 carries out the thermal stress of high-rise buildings, and comes up with the suggestions on the structural design and optimization of these buildings.

2. THERMAL STRESS ANALYSIS

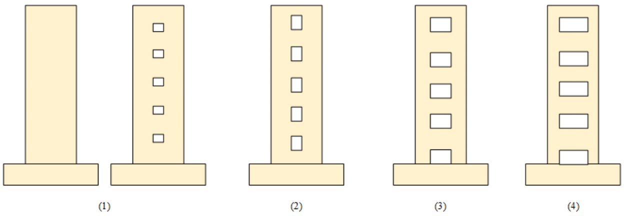

Figure 1. Structural types of high-rise buildings

Figure 1 shows the four structural types of high-rise buildings, namely, integrated structure, small-opening wall structure, coupled shear wall structure, and wall-frame structure. The stack effect refers to the enhancement of indoor convection by the upward or downward flow of the indoor air along the vertical slopes. This effect is a common form of heat exchange in high-rise buildings, due to the vertical circulation spaces like the shared atrium, vertical air shafts, and staircases. The stack effect is especially prominent in integrated structures with small and narrow openings on the walls. Driven by the temperature difference in the circulation spaces, the fluid will diffuse along the space under the stack effect.

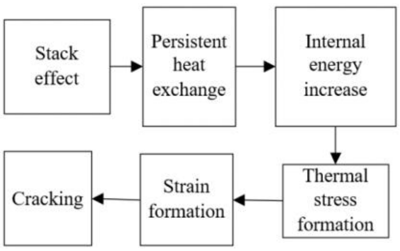

Figure 2. Cracking mechanism of structural members in high-rise buildings under stack effect

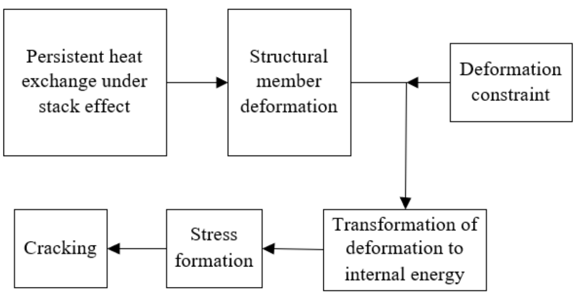

Figure 3. Cracking mechanism of structural members in high-rise buildings under deformation constraint

Figures 2 and 3 explains the cracking mechanism of structural members in high-rise buildings under stack effect. It can be seen that the stack effect has a certain impact on the structural members of such buildings. Regardless of the deformation constraint, the persistent heat exchange may cause the structural members to deform, and eventually crack. The thermal shrinkage stress of the walls of high-rise buildings depends on the boundary constraints, and the variation of temperature and humidity. To prevent and control the cracking of the structural members in high-rise buildings, and to ensure building quality, this paper explores the thermal stress of the structural members in high-rise buildings through finite-element analysis, in the light of the stack effect.

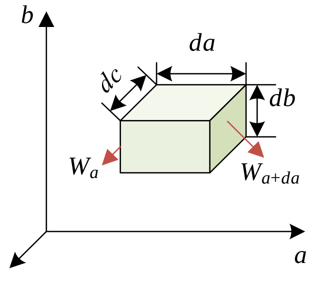

Figure 4. Unit heat flow in the structural member

The concrete structural members in high-rise buildings can be regarded as elastic bodies. Before computing the thermal shrinkage stress, it is necessary to first split each member into multiple units. Figure 4 illustrates the unit heat flow in the structural member. Let $\{\varphi\}$ be the unit stress of the member; $[E]$ be the elastic matrix; $\{\rho\}$ be the unit strain of the member; $[Y]$ be the strain transformation matrix; $\{\rho_0\}$ be the initial strain caused by temperature variation. For a mass point in the structural member, $\{\varphi\}$ can be expressed as:

$$\{\phi\}=[E](\{\rho\}-\{\rho_0\})=[E][Y]-[E]\{\rho_0\} \tag{1}$$

Let β be the linear expansion coefficient of concrete; ψ be the temperature change of concrete side walls; $\{\}^T$ be the node displacement of member unit. Then, $\{\varphi\}$ can be expressed as:

$$\{\rho_0\}=\{\rho_a\rho_b\rho_{ab}\}\psi=\beta\psi\{110\}^T \tag{2}$$

According to the principle of virtual work, the virtual work produced by external stress is equal to that produced by internal stress. Therefore, it can be inferred that the concrete structural members of high-rise buildings, which are regarded as elastic bodies, are in equilibrium state under the action of external forces. Let $\{\xi\}$ be the virtual displacement generated by a member unit d. Then, the virtual work done by the stress is the product between the stress on the unit node and its virtual displacement:

$$Q_1=\{\bar{\xi}\}^T\{G\}^d \tag{3}$$

Substituting $[Y]$ into formula (3), the virtual strain corresponding to the virtual displacement $\{\xi\}^T$ can be calculated by:

$$\{\bar{\rho}\}=[Y]\{\bar{\xi}\} \tag{4}$$

In the member unit, it is assumed that the unit thickness is 1. Then, the virtual work done by the internal stress at this time can be calculated by:

$$Q_2 = \iint \{\bar{\rho}\}^T \{\phi\} dadb \tag{5}$$

Through matrix operation, the following equation can be obtained:

$$\{\bar{\rho}\}^T = \left([Y]\{\bar{\xi}\}\right)^T = \{\bar{\xi}\}^T [Y]^T \tag{6}$$

Without considering the initial strain of the member unit, the following can be derived from formula (1):

$$\{\phi\} = [E]\{\rho\} = [E][Y]\{\phi\}^d \tag{7}$$

Combining formulas (5)-(7), the internal virtual work produced by the virtual displacement of the member unit can be calculated by:

$$Q_2 = \{\bar{\xi}\}^T \left(\iint [Y]^T [E][Y] dadb\right)\{\xi\}^d \tag{8}$$

According to the principle of virtual work, the value of Q_1 calculated by formula (3) is equal to the value of Q_2 calculated by formula (5). Thus, we have:

$$\{\bar{\xi}\}^T \{G\}^d = \{\bar{\xi}\}^T \left(\iint [Y]^T [E][Y] dadb\right)\{\xi\}^d \tag{9}$$

Formula (9) holds for the virtual displacement of any unit in the structural members in the high-rise buildings. Let $[l]$ be the stiffness matrix; $\{G\}^d$ be the node force induced by the node displacement of the structural member. Formula (9) can be transformed into:

$$\begin{aligned} &\{G\}^d = [l]\{\xi\}^d \\ &[l] = \iint [Y]^T [E][Y] dadb \end{aligned} \tag{10}$$

Without considering the influence of external environment, the structural member deformation of high-rise buildings induced by the heat exchange under the stack effect can be regarded as the initial strain. Combining formulas (1) and (5), the virtual work produced by the virtual displacement of the member unit can be calculated by:

$$\begin{aligned} Q_2 &= \iint \{\bar{\rho}\}^T \{\phi\} dadb \\ &= \{\bar{\xi}\}^T \left([l]\{\xi\}^d - \iint [Y]^T [E]\{\rho_0\} dadb\right) \end{aligned} \tag{11}$$

According to the virtual work principle, we have:

$$\begin{aligned} &\{\bar{\xi}\}^T \{G\}^d \\ &= \{\bar{\xi}\}^T \left([l]\{\xi\}^d - \iint [Y]^T [E]\{\rho_0\} dadb\right) \end{aligned} \tag{12}$$

Let $\{G_0\}^d$ be the node force of the member unit induced by the initial strain; $[K]$ be the $\iint[Y]^T[E]\{\rho_0\}dadb\{\rho_0\}$; $\{\rho_0\}$ be the initial strain. Then, the following transformation can be established:

$$\begin{aligned} &\{G\}^d = [l]\{\xi\}^d + \{G_0\}^d \\ &[G_0] = -\iint [Y]^T [E]\{\rho_0\} dadb = [K]\{\rho_0\} \end{aligned} \tag{13}$$

Since $\{\rho_0\}$ is the thermal strain, we have $\{G_0\}^d=\{G_\psi\}^d$. Without considering the stress effect of other loads, the above formula can be converted into:

$$[l]^d \{\xi\}^d = [K]\{\rho^T\} \tag{14}$$

Summing up the member units of the entire high-rise building, we have:

$$[l]\{\xi\} = [K]\{\rho^T\} \tag{15}$$

After acquiring $\{\xi\}$, it is possible to compute the thermal stress of each member unit. When the temperature load of a high-rise building is fixed, the thermal shrinkage stress of the building can be equivalent to the continuous increment of thermal stress of each unit in a period. Adding up the thermal stress increment of each unit, the total thermal stress of high-rise buildings can be obtained as:

$$\begin{aligned} \{\Delta\phi\} &= [E]\left(\{\Delta\rho\} - \{\Delta\rho_0\}\right) \\ &= [E][Y]\{\Delta\xi\}^d - [E]\{\Delta\rho_0\} \end{aligned} \tag{16}$$

3. FINITE-ELEMENT CALCULATION

For structural members of high-rise buildings, the main mechanical properties include compressive strength, tensile strength, elastic modulus, and ultimate tensile deformation. Since the concrete structural members of high-rise buildings are usually regarded as elastic bodies, their elastic creep properties must be fully considered to compute their instantaneous thermal stress fields. Let $\rho(o)$ be the total deformation of the structural member facing the heat exchange under the stack effect; $\rho_1(o)$ be the creep deformation related to the age, duration under stress load, and stress level of the structural member; $\rho_2(o)$ be the instantaneous strain induced by the stress; $\rho_3(o)$ be the dry shrinkage deformation caused by water loss of the structural member; $\rho_4(o)$ be the autogenous volume deformation; $\rho_5(o)$ be the thermal deformation indued by heat exchange under the stack effect. Then, the total deformation of the concrete structural member in a high-rise building induced by the persistent heat exchange under the stack effect can be calculated by:

$$\begin{aligned} \rho(o) &= \rho_1(o) + \rho_2(o) \\ &+ \rho_3(o) + \rho_4(o) + \rho_5(o) \end{aligned} \tag{17}$$

For the structural member of a high-rise building, the stress increment is denoted as $\{\Delta\rho_m\}$; the corresponding creep strain increment is denoted as $\{\Delta\rho_{m1}\}$; the elastic strain increment is denoted as $\{\Delta\rho_{m2}\}$; the dry shrinkage strain increment is denoted as $\{\Delta\rho_{m3}\}$; the temperature strain increment is denoted as $\{\Delta\rho_{m5}\}$; the autogenous volume strain increment is denoted as $\{\Delta\rho_{m4}\}$. Then, the strain increment of the structural member can be calculated by:

$$\{\Delta\rho_m\} = \{\Delta\rho_{m1}\} + \{\Delta\rho_{m2}\} + \{\Delta\rho_{m3}\} + \{\Delta\rho_{m5}\} + \{\Delta\rho_{m6}\} \tag{18}$$

$\{\Delta\rho_{m2}\}$ can be calculated by:

$$\{\Delta\rho_{m2}\} = \frac{1}{D\left(o_m^*\right)}[W][\Delta\phi_m] \tag{19}$$

where,

$$[W] = \begin{bmatrix} 1 & -\lambda & -\lambda & 0 & 0 & 0 \\ & 1 & -\lambda & 0 & 0 & 0 \\ & & 1 & 0 & 0 & 0 \\ & & & 2(1+\lambda) & 0 & 0 \\ & & & & 2(1+\lambda) & 0 \\ & & & & & 2(1+\lambda) \end{bmatrix} \tag{20}$$

The elastic modulus $D(o_m^*)$ satisfying $o_m^*=(o_{m-1} + o_m)/2$ can be estimated by:

$$D(o) = D_0\left[1 - exp\left(-xo^y\right)\right] \tag{21}$$

$$D(o) = \frac{D_0 o}{w + o} \tag{22}$$

The creep strain increment of the structural member can be calculated by:

$$\{\Delta\rho_{m1}\} = \{\delta_m\} + RE\left(p_m, o_m^*\right)[W]\{\Delta\phi_m\} \tag{23}$$

where,

$$\{\delta_m\} = \sum_r \left(1 - d^{-s_r\Delta o_m}\right)\{\theta_{rm}\} \tag{24}$$

$$\{\theta_{rm}\} = \{\theta_{r,m-1}\} d^{-s_r\Delta o_{m-1}} + [W]\{\Delta\phi_{m-1}\} \Phi_r\left(o_{m-1}^*\right) d^{-0.5 s_r \Delta o_{m-1}} \tag{25}$$

$$RE\left(p_m, o_m\right) = \sum_r \Phi_r(\tau)\left[1 - d^{-\alpha_r(p-o)}\right] \tag{26}$$

Let κ be the linear expansion coefficient of the structural member; $\Delta\psi_m$ be the temperature variation induced by the persistent heat exchange under the stack effect. Based on the non-steady thermal stress field solved for the structural member in a high-rise building, the temperature strain increment $\{\Delta\rho_{m5}\}$ induced by the persistent heat exchange under the stack effect can be calculated by:

$$\{\Delta\rho_{m5}\} = \{\kappa\Delta\psi_m, \kappa\Delta\psi_m, \kappa\Delta\psi_m, 0, 0, 0\}^T \tag{27}$$

Let $\{\rho_{m0}\}$ be the final dry shrinkage strain of the structure. Then, the dry shrinkage increment can be calculated by:

$$\{\Delta\rho_{m3}\} = \{\rho_{m3}\} - \{\rho_{m_3-1}\} \tag{28}$$

$$\{\rho_{m3}\} = \{\rho_{m0}\} - \left\{1 - d^{-uo_m^e}\right\} \tag{29}$$

Based on the basic assumptions of elastic creep theory, the increment of the structural member in any period Δp can be expressed as:

$$\{\Delta\phi_m\} = \left(\overline{E_m}\right)\begin{pmatrix} \{\Delta\xi_m\} - \{\delta_m\} \\ -\{\Delta\rho_m^T\} - \{\Delta\rho_{m0}\} - \{\Delta\rho_{m3}\} \end{pmatrix} \tag{30}$$

$$[E_m] = D_m[W]^{-1} \tag{31}$$

$$\overline{D_m} = \frac{D\left(o_m^*\right)}{1 + D\left(o_m^*\right)RW \cdot D\left(p_m, o_m^*\right)} \tag{32}$$

The node force of a member unit can be calculated by:

$$\{\Delta G\}^d = \iiint [Y]^T \{\Delta\xi_m\} dadbdc \tag{33}$$

The calculated $\{\Delta\varphi_m\}$ can be combined with formula (33):

$$\{\Delta G\}^d = [l]^d \{\Delta\xi_m\}^d - \iiint [Y]^T \left[\overline{E_m}\right]\begin{pmatrix} \{\delta_m\} + \{\Delta\rho_{m5}\} \\ + \{\Delta\rho_{m0}\} + \{\Delta\rho_{m3}\} \end{pmatrix} dadbdc \tag{34}$$

The stiffness matrix $[l]^d$ of the member unit can be obtained by:

$$[l]^d = \iiint [Y]^T \left[\overline{E_m}\right][Y] dadbdc \tag{35}$$

The second term of formula (34) is the node force of the structural member induced by non-stress deformation. The corresponding load increment of the member unit can be expressed by formulas (36)-(39).

The load increments $\{\Delta V_m\}_{d1}$, $\{\Delta V_m\}_{d3}$, $\Delta V_m\}_{d4}$, and $\{\Delta V_m\}_{d5}$ induced by creep deformation, dry shrinkage, autogenous volume deformation, and temperature variation can be respectively calculated by:

$$\{\Delta V_m\}_{d1} = \iiint [Y]^T \left[\overline{E_m}\right]\{\delta_m\} dadbdc \tag{36}$$

$$\{\Delta V_m\}_{d3} = \iiint [Y]^T \left[\overline{E_m}\right]\{\Delta\rho_{m3}\} dadbdc \tag{37}$$

$$\{\Delta V_m\}_{d4} = \iiint [Y]^T \left[\overline{E_m}\right]\{\Delta\rho_{m4}\} dadbdc \tag{38}$$

$$\{\Delta V_m\}_{d5} = \iiint [Y]^T \left[\overline{E_m}\right]\{\Delta\rho_{m5}\} dadbdc \tag{39}$$

Let $[\Psi]$ be the stiffness matrix; $\{\Delta\varphi_m\}$ be the node displacement increment of structural member; $\{\Delta V_m\}_0$, $\{\Delta V_m\}_1$, $\{\Delta V_m\}_3$, $\{\Delta V_m\}_4$, and $\{\Delta V_m\}_5$ be the node load increments induced by creep deformation, dry shrinkage, autogenous volume deformation, and temperature variation, respectively. Then, the overall equilibrium equation of the member node in a high-rise building can be expressed as:

$$[\Psi]\{\Delta\xi_m\} = \{\Delta V_m\}_0 + \{\Delta V_m\}_1 + \{\Delta V_m\}_5 + \{\Delta V_m\}_6 + \{\Delta V_m\}_3 \tag{40}$$

For any member node, the load increment is the superposition of the load increments of the surrounding nodes. By formula (40), it is possible to solve the displacement increment $\{\Delta\xi_m\}$ of each member node, and thus the stress increment $\{\Delta\varphi_m\}$ of each node. Then, the total stress of each unit can be obtained by accumulating the stress increments:

$$\{\phi_m\} = \{\Delta\phi_1\} + \{\Delta\phi_2\} + \ldots + \{\Delta\phi_m\} = \sum\{\phi_m\} \tag{41}$$

4. EXPERIMENTS AND RESULTS ANALYSIS

Table 1. Temperature rise of structural members in high-rise buildings

	Wall thickness	Temperature rise	Mean temperature	Highest temperature
Hot weather	0.6	7	30~36	35~47
	1.2	12	31~37	34~45
	2.4	22	30~35	38~46
	3.6	34	32~38	35~48
	4.2	41	31~36	36~46
	Wall thickness	**Temperature rise**	**Mean temperature**	**Highest temperature**
Cold weather	0.6	6	11~17	16~22
	1.6	10	9~12	20~25
	2.6	17	13~19	29~36
	3.6	28	8~14	35~41
	4.6	35	12~18	47~53

In cold weather, the structural members of high-rise buildings are basically elastic or elastoplastic, with a small temperature stress and a small elastic modulus. Under the stack effect, the temperature stress and elastic modulus of each member quickly increase. When the restraining stress surpasses the tensile strength of the member, cracking will occur. The theory on the persistent heat exchange under the stack effect is rather complex. Owing to the variation of internal circulation space within high-rise buildings, the theoretical result differs from the actual engineering result to a certain extent. Table 1 lists the temperature rise of structural members in high-rise buildings. The data in the table are measured by the following conditions: 255 kg of blast furnace slag cement is used in each cubic meter of structural member, under the steel structure framework. The data in Table 1 need to be modified according to the type of cement.

Figures 5 and 6 compare the measured and theoretical surface temperatures and thermal stresses of the structural member. The two sets of curves show that the measured surface temperature of the structural member differed slightly from the theoretical temperature, and the goodness-of-fit was very high. The temperature stress did not change greatly, exhibiting an inverted U-shaped trend. The theoretical results were close to the engineering results.

Table 2 shows the increments of thermal stress and strain of structural members at different ages. It can be seen that, with the elapse of time, the elastic modulus of the structural members in high-rise buildings continued to increase, while the thermal strain and thermal stress of the structural members first increased and then decreased. Through accumulation, the total thermal stress of the structural members can be obtained, making it possible to predict member cracking.

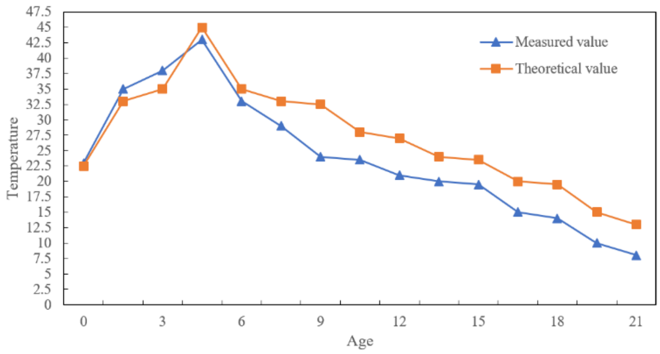

Figure 5. Measured and theoretical surface temperatures of the structural member

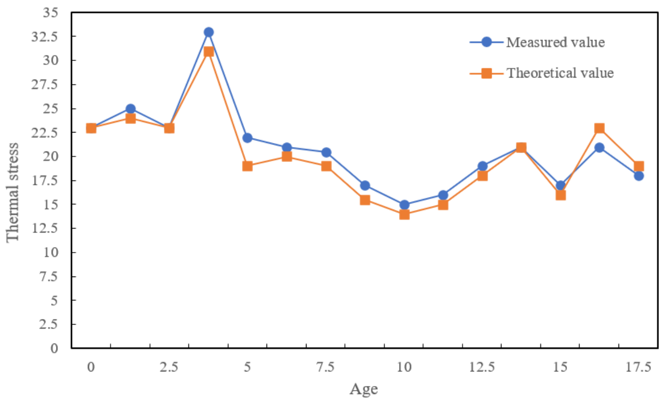

Figure 6. Measured and theoretical thermal stresses of the structural member

Table 2. Increments of thermal stress and strain of structural members at different ages

Age	1	2	3	4	5	6
Temperature difference	13.05	9.18	7.04	3.68	2.46	0.93
Elastic modulus	0.517	0.749	0.972	1.046	1.482	1.791
Thermal strain increment	2.084×10^{-4}	1.806×10^{-4}	1.958×10^{-4}	1.261×10^{-4}	1.719×10^{-4}	1.696×10^{-4}
Thermal stress increment	0.481	0.435	0.402	0.268	0.175	0.092

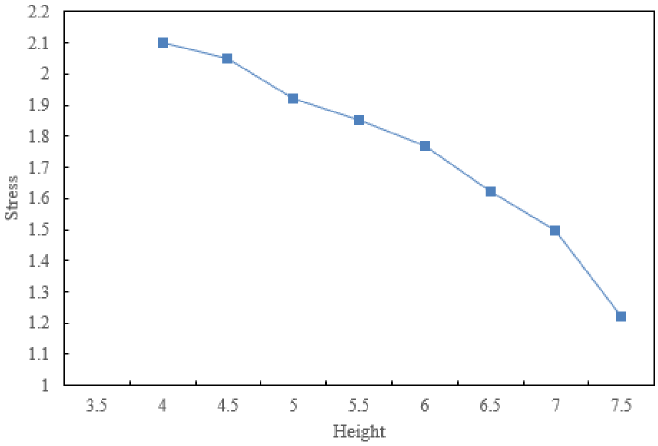

Figure 7. Relationship between thermal stress and the height of high-rise buildings

Without changing the wall length, wall thickness, and member strength of high-rise buildings, this paper carries out thermal stress analysis on structural members of different heights, with the aid to disclose the law of wall height affecting the thermal stress on structural members. Figure 7 presents the relationship between thermal stress and the height of high-rise buildings. Before finite-element modeling, the model heights were set to 3.5 m, 4 m, 4.5 m, 5 m, 5.5 m, 6 m, 6.5 m, 7 m, and 7.5 m, respectively, and the other boundary conditions were fixed. It can be seen that the thermal stress gradually declined with the rising height of the building.

Drawing on the above findings, this paper optimizes the structural members of high-rise buildings. Table 3 shows the optimization results on different performance indices of the simulation model.

As shown in Table 3, the maximum interlayer displacement angles of the optimized simulation model met the requirements in relevant codes, i.e., the optimized model has a relatively good lateral stiffness. For high-rise buildings with active high-order vibration modes, the stiffness degradation and thermal stress response under the high temperature are complicated by the stack effect. It can be seen from Table 3 that the high-temperature thermal stress is negatively correlated with the stack effect, and positively with wall thickness and member strength level. The ratio of high-temperature stress to low-temperature stress also met the requirements of thermal stress analysis on structural members. Finally, Figure 8 presents the proportion of thermal stress for the structurally optimized high-rise building. It can be seen that the minimum thermal stress was 1.22% of the optimization scheme. Hence, the horizontal and lateral proportions of thermal stress in the scheme both satisfy the limits prescribed in relevant codes.

Table 3. Optimization results on performance indices

Wall thickness		2.0			3.0		
Strength level		31	36	41	31	36	41
Maximum interlayer displacement angle	Lateral	1/302	1/328	1/361	1/374	1/328	1/384
	Horizontal	1/617	1/638	1/641	1/691	1/749	1/835
High-temperature thermal stress	Lateral	5154.6	5349.1	5617.3	5674.6	5394.2	5648.5
	Horizontal	5192.8	5481.4	5647.2	6234.5	6027.3	6594.8
Low-temperature thermal stress	Lateral	1375.1	1296.7	1327.5	1695.7	1165.2	1679.3
	Horizontal	1412.7	1537.5	1274.9	1985.2	1438.5	1329.4

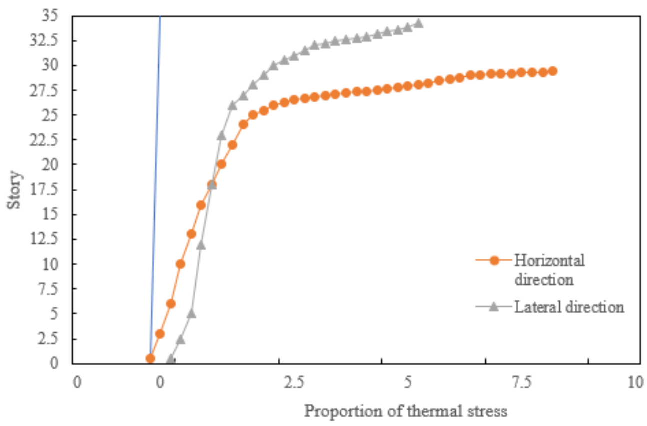

Figure 8. Proportion of thermal stress

5. CONCLUSIONS

This paper analyzes the thermal stress and optimizes the structure of high-rise buildings under stack effect. Firstly, the authors expounded on the cracking mechanism of structural members in high-rise buildings under stack effect, before analyzing the thermal stress of these buildings induced by that effect. Then, the instantaneous stress field of high-rise buildings was solved through finite-element calculation. Through experiments, the temperature rise of structural members in high-rise buildings was summarized, and the measured surface temperature and thermal stress of structural members were compared with the theoretical values. In this way, it is concluded that, with the elapse of time, the thermal strain and thermal stress of structural members first increase and then decline. Furthermore, the authors recorded the increments of thermal stress and strain of structural members at different ages, and plotted the relationship between thermal stress and the height of high-rise buildings. The results show that the thermal stress gradually declines with the growing building height. Finally, the optimization results on different performance indices of the simulation model were summarized, revealing that the horizontal and lateral proportions of thermal stress in the scheme both satisfy the limits prescribed in relevant codes. Besides, several suggestions were provided for the structural design and optimization of high-rise buildings.

ACKNOWLEDGEMENTS

Supported by the key project of Provincial Natural Science Foundation of Anhui Universities "Research on green construction strategy of Huizhou traditional human settlements from the perspective of Rural Revitalization" (Grant No.: KJ2021A1153).

REFERENCES

[1] Huang, D.M., Zhu, L.D., Ding, Q.S., Zhu, X., Chen, W. (2017). Aeroelastic and aerodynamic interference effects on a high-rise building. Journal of Fluids and Structures, 69: 355-381. https://doi.org/10.1016/j.jfluidstructs.2017.01.007

[2] Kern, A.P., Amor, L.V., Angulo, S.C., Montelongo, A. (2018). Factors influencing temporary wood waste generation in high-rise building construction. Waste Management, 78: 446-455. https://doi.org/10.1016/j.wasman.2018.05.057

[3] Fan, Y., Li, Y., Hang, J., Wang, K., Yang, X. (2016). Natural convection flows along a 16-storey high-rise building. Building and Environment, 107: 215-225. https://doi.org/10.1016/j.buildenv.2016.08.003

[4] Xie, X.D., Wang, Q. (2016). Design of a piezoelectric harvester fixed under the roof of a high-rise building. Engineering Structures, 117: 1-9. https://doi.org/10.1016/j.engstruct.2016.03.018

[5] Zou, X., Wang, Z.S., Li, Z.L. (2016). Experimental study on the wind load characteristics of high-rise building in stationary downbursts. Hunan Daxue Xuebao/Journal of Hunan University Natural Sciences, 43(1): 29-36.

[6] Cho, H.P., Lim, H., Lee, D., Cho, H., Kang, K.I. (2018). Patent analysis for forecasting promising technology in high-rise building construction. Technological Forecasting and Social Change, 128: 144-153. https://doi.org/10.1016/j.techfore.2017.11.012

[7] Yu, X., Xie, Z., Li, S., Wang, X. (2017). Interference effect of wind-induced internal pressure for super high-rise building with opening. Jianzhu Jiegou Xuebao/Journal of Building Structures, 38(10): 95-101.

[8] Zhao, G., Beji, T., Merci, B. (2017). Study of FDS simulations of buoyant fire-induced smoke movement in a high-rise building stairwell. Fire Safety Journal, 91: 276-283. https://doi.org/10.1016/j.firesaf.2017.04.005

[9] Xie, W. (2017). Incorporating building information modeling (BIM) into the super high-rise industrialized housing project: A case study. Boletín Técnico, 55(13): 234-243.

[10] Feng, H.H., Wang, X. (2011). Causes and control measures of mass concrete crack of high-rise building basement foundation slab. In Advanced Materials Research, 163: 1609-1613.

[11] Guo, J.J., Wang, W. (2010). Methods for crack prevention of large volume concrete foundation of high-rise building. In Applied Mechanics and Materials, 29: 305-309.

[12] Ola, F.B., Sekarlangit, N., Michelle, B., Anindita, M.D.K.A., Setyaningfebry, F.U. (2021). Heat transfer in the universal form of high-rise buildings in various climate zones. Journal of Applied Science and Engineering, 25(1): 187-194. https://doi.org/10.6180/jase.202202_25(1).0019

[13] Derzsi, I., Takács, J. (2019). Hydraulic analyze of risers of heating system in high-rise building. Periodica Polytechnica Mechanical Engineering, 63(2): 156-163. https://doi.org/10.3311/PPme.13320

[14] Song, D., Yoon, S., Jeong, C., Kim, J., Lim, H. (2019). Heat, vapor, and CO_2 transportation caused by airflow in high-rise residential buildings. Building and Environment, 160: 106176. https://doi.org/10.1016/j.buildenv.2019.106176

[15] Aksenov, A., Malysheva, A. (2018). Calculation of critical heat transfer in horizontal evaporator pipes in cooling systems of high-rise buildings. In E3S Web of Conferences, 33: 02037. https://doi.org/10.1051/e3sconf/20183302037

[16] Ha, P.T.H. (2018). Energy efficiency façade design in high-rise apartment buildings using the calculation of solar heat transfer through windows with shading devices. In IOP Conference Series: Earth and Environmental Science, 143(1): 012055. https://doi.org/10.1088/1755-1315/143/1/012055

[17] Bak, J., Koo, J., Yoon, S., Lim, H. (2022). Thermal draft load coefficient for heating load differences caused by stack-driven infiltration by floor in multifamily high-rise buildings. Energies, 15(4): 1386. https://doi.org/10.3390/en15041386

[18] Kim, D.D., Suh, H.S. (2021). Heating and cooling energy consumption prediction model for high-rise apartment buildings considering design parameters. Energy for Sustainable Development, 61: 1-14. https://doi.org/10.1016/j.esd.2021.01.001

[19] Bak, J., Yoon, S. (2021). Dwelling infiltration and heating energy demand in multifamily high-rise and low-energy buildings in Korea. Renewable and Sustainable Energy Reviews, 148: 111284. https://doi.org/10.1016/j.rser.2021.111284

[20] Shi, W.X., Ji, J., Sun, J.H., Lo, S.M., Li, L.J., Yuan, X.Y. (2014). Influence of staircase ventilation state on the airflow and heat transfer of the heated room on the middle floor of high rise building. Applied Energy, 119: 173-180. https://doi.org/10.1016/j.apenergy.2013.12.055

[21] Xi, R. (2017). Design and research on the functions of energy saving and heat preservation in high-rise buildings. Agro Food Industry Hi-Tech, 28(1): 1573-1577.

[22] Qi, D., Wang, L.L., Zhao, G. (2017). Froude-Stanton modeling of heat and mass transfer in large vertical spaces of high-rise buildings. International Journal of Heat and Mass Transfer, 115: 706-716. https://doi.org/10.1016/j.ijheatmasstransfer.2017.08.030

[23] Guo, L. (2019). Formation of temperature cracks of concrete in high-rise buildings and the corresponding measures. Archives of Civil Engineering, 65(4): 177-188. https://doi.org/10.2478/ace-2019-0053

[24] Russell, H.G. (1987). High-Rise concrete buildings: Shrinkage, Creep, and temperature effects. Special Publication, 97: 125-138.

[25] Khan, F.R., Fintel, M. (1971). Conceptual details for creep, shrinkage, and temperature in ultra high-rise buildings. Special Publication, 27: 215-228.

[26] Kahsay, M.T., Bitsuamlak, G., Tariku, F. (2020). Effect of localized exterior convective heat transfer on high-rise building energy consumption. In Building Simulation, 13(1): 127-139. https://doi.org/10.1007/s12273-019-0568-7